Experimental report

02/07/2024

Proposal: 9-13-1061 **Council:** 10/2022

Title: Location of Enzymes in a Polymersome

Research area: Soft condensed matter

This proposal is a continuation of 9-12-644

Main proposer: Albena LEDERER

Experimental team: Zahn STANVLIET
Upenyu MUZA
Kehu ZHANG

Local contacts: Ralf SCHWEINS

Samples: PEO-copolymers

Instrument	Requested days	Allocated days	From	To
D22	3	1	28/05/2023	29/05/2023

Abstract:

Polymersomes are fabricated using self-assembly of amphiphilic block copolymers to multicompartment-capsules, and hold great promise as synthetic cells, to mimic cell functions and in the diagnostics and therapeutics of different diseases. However, complete knowledge of the molecular processes for the encapsulation and release of nanometer-sized biomolecules from tunable multiresponsive polymersomes within the physiological pH range of 4-8 is still required. Preliminary SANS measurements at ILL were performed with deuterated cargo protein in D2O. The results confirm TEM results showing an increased thickness of the membrane due to interaction with the protein. With these measurements, we were only able to determine the changes in the membrane thickness after encapsulation, but not to identify the membrane conformation changes depending on pH. Yet, an essential breakthrough in understanding the exact location of the cargo is expected by using selective deuteration and different contrast in the hydrophobic core and the hydrophilic shell of the membrane.

Report for ILL proposal 9-13-1061: Location of Enzymes in a Polymersome

As a powerful nondestructive analytical tool for analysing soft materials, SANS was used to investigate the structure of un-loaded and loaded polymersome particles (Psomes). The permeation of the Psomes membrane can be controlled be changing the pH: low pH - open vs high pH - closed (collapsed) membrane. Beyond previous investigations on these systems, the location of the cargo within the polymersome should be elucidated further (Figure 1). Additionally, by using the deuterated analogue of the block copolymer (Dsome) contrast within the Dsome shell should be increased to allow for a detailed modelling of the expected three-layered shell system to get even deeper insight into the interaction of cargo with the polymer particle.
Psomes were prepared by co-assembly of amphiphilic block copolymer mixtures and subsequent crosslinking by exposure to UV light. The biocompatible, non-immunogenic block copolymers are composed of (i) hydrophilic block: poly(ethylene glycol) and (ii) hydrophobic block: diethyl amino ethyl methacrylate, dimethyl amino ethyl methacrylate (DMAEMA) (pH-sensitive segments), and 3,4-dimethyl maleic imidobutyl methacrylate (photo-cross-linking segment) (Figure 1). Deuterated analogue of this block copolymer (Dsome) was prepared by d_5-DMAEMA monomers in the hydrophobic block to allow for selective contrast matching of internal and external parts of the Psome membrane.

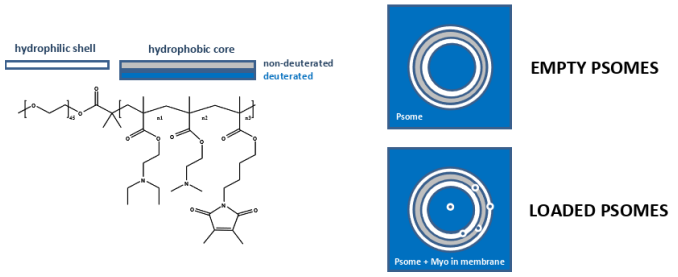

Figure 1: Chemical structure and concept of the block-copolymers used for Psome and Dsome formation (left), and scheme of the three-component shell of the Psome (right) with and without cargo in D_2O

The scattering intensities of empty Psomes and Dsomes were tested at concentrations of 0.1, 0.2 and 0.5 mg/mL to determine optimal measurement parameters. A concentration of 0.2 mg/mL was selected for subsequent experiments as the optimal concentration for sufficient scattering intensity while a significant aggregation signature in the SANS data was still absent. The pH was set to 8, ensuring collapsed Psome's membrane.

It is well known that polydispersity has to be considered for the evaluation of SANS data of these systems.[1–3] Thus, dynamic light scattering (DLS) experiments were performed for concentrated Psome solutions (concentration of 0.5 mg/mL or 1 mg/mL) at the ILL directly before the SANS measurements. An average PDI of the empty Psomes of 0.3 ± 0.1 was obtained and used as the initial polydispersity parameter in the SANS modelling.

Empty Psomes and Dsomes

Modelling of empty Psomes in D_2O was done with the core-shell model, implemented in SASView, additionally utilizing a hard-sphere structure factor and an averaged scattering length density (SLD) of 1.76 10^{-6} Å^{-2} of the shell (core SLD equal to the SLD of D_2O). A very good agreement of model and SANS data was obtained ($\chi^2 = 11$) (Figure 2A) by considering the polydispersity of the core radius and shell thickness of 0.3. Without a shell thickness polydispersity, the fit quality was reduced to $\chi^2 = 26$. Since the Psomes interior is not purified from unreacted block-copolymers after the Psome formation a further aggregation of unbound block-copolymers onto the Psome shell could be possible upon collapsing the Psomes membrane at pH 8, potentially leading to the observed polydispersity of the shell thickness. Additionally, measurements were performed with a low buffer concentration. Thus, charges are not fully screened and electrostatic interaction might have to be considered. Modelling the empty Psome with a sticky sphere structure factor to consider such interaction was performed for comparison, leading to further improvement of the fit quality ($\chi^2 = 9$). Since there was less variation

in fit parameters between the use of the two structure factors, results in this report will be obtained with the hard-sphere structure factor. Psome sizes in D_2O were determined to (24.0 ± 0.1) nm for the core radius and (11.5 ± 0.1) nm for the shell thickness, leading to a total diameter of the Psomes of ca. 50 nm, which is in good agreement with sizes reported by other methods.[4]

In a next step, a modelling of the substructure of the shell was attempted by a core – three-layer shell model, using pre-calculated SLDs based on the structural formula of hydrophilic and hydrophobic blocks and considering a swelling degree of 2 of the hydrophilic PEG block. However, the data quality did not allow for further refining of the model. Sub-thicknesses of the shell run into zero in the fit leading to an average shell model as discussed before.

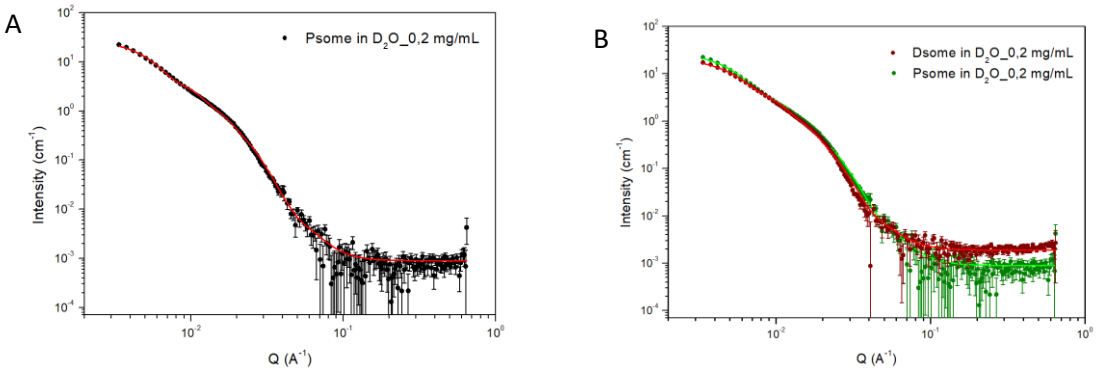

Figure 2: A: Modeling of SANS data of empty Psome in D_2O utilizing a core-shell model. Polydispersity of core radius and shell thickness was considered, both values fixed at 0.3. A final core size of (24.0 ± 0.1) nm and shell thickness of (11.5 ± 0.1) nm were obtained. B: Comparison between modeling of SANS data of empty Psome in D_2O (green) and empty Dsome in D_2O (red) utilizing a core-shell model.

Modeling of the empty 50% Dsomes was performed with the same evaluation strategy as for the Psomes, and the core-shell modell with hard-sphere structure factor provided the best fit ($\chi^2 = 10$) with a core radius of (24.4 ± 0.1) nm and a shell thickness of (12.8 ± 0.1) nm. These results are very similar to the findings for the empty Psome. Although the signal-to-noise ratio of the 50% Dsome SANS data is considerably better than for the empty Psome, more insight into the shell sub-structure by utilizing the more complex core – three-layer shell model is not likely due to the absence of characteristic features in the SANS data in the mid-q-range (Figure 2B). We consider the high polydispersity in the Psome as well as in the Dsome system to be detrimental to the intended further structure elucidation of the shell. A more advanced purification procedure of the Psome structures to reduce presumably the PDI of the shell thickness is already in the test phase. Further separating the Psomes before SANS experiments by an advanced separation technique, e.g. AF4, will help to reduce PDI of the Psome radius, and perspectively could provide the necessary system purification for improved SANS data and further structure elucidation.

Loading of Psomes with Cargo

For the evaluation of loaded Psomes the core-shell model of the unloaded Psomes was used as the starting point. All parameters were fixed, except the size parameters (core radius and shell thickness) and the SLDs. Also for the loaded Psomes the core-shell model worked well, with fit χ^2 values between 13 and 16 for the different cargos Myoglobin (MYO), Hyaluronidase (HYAL) and gold nanoparticles (Au NPs). For all types of cargo, the thickness of the shell increased while the SLD of the shell decreased (Table 1). Additionally, the SLD of the core did not change from the SLD of D_2O in the modelling. Since the calculated SLDs of the different cargos were lower than the calculated shell SLD, we conclude that all types of cargo are bound to the shell but do not enter the core of the Psomes. Binding to the shell in a post-loading process is expected to some extent. However, it was surprising that no cargo could pass the swollen shell in the loading process at pH 6 to enter the core. Sizes of MYO and HYAL were

analyzed from reference SANS data (Table 1), while for the Au NPs a particle size of 5 nm with an absolute diameter of 11 nm including the citrate shell was considered as reported by the supplier. From the SANS data of MYO, aggregation of the protein in solution is likely and might lead to the observed unique loading of the shell since aggregates are not able to enter into the Psome core. For HYAL, aggregation in solution was not obvious but can also not be completely excluded based on the present data. A low-salted buffer was chosen for the experiments since the Au NPs are known to aggregate at higher salt concentrations. Nevertheless, a delicate tuning of buffer conditions considering the iso-electric point of the specific cargo will be considered in the future.

Table 1: Structural data of cargo (sphere-model) and loaded Psomes (core-shell model) as extracted from modelling of SANS data. *The size of Au NPs was not measured individually but was taken from the supplier.

Cargo	Diameter [nm]	Psome core radius [nm]	Psome shell thickness [nm]	Psome shell SLD [10^{-6} Å^{-2}]	SLD solvent [10^{-6} Å^{-2}]
MYO	3.6 ± 0.2	24.6 ± 0.1	14.0 ± 0.1	1.385 ± 0.006	5.702 ± 0.009
HYAL	4.0 ± 0.3	21.6 ± 0.1	13.6 ± 0.1	1.118 ± 0.007	5.35 ± 0.01
Au NPs	5*	23.8 ± 0.1	13.8 ± 0.1	1.506 ± 0.006	5.626 ± 0.009

Experimental details

SANS measurements were carried out at instrument D22 of the Institut Laue-Langevin (ILL, Grenoble) at a constant temperature of 293 K. The neutron wavelength was set to 6 Å. A broad q-range from 0.0033 Å^{-1} – 0.64 Å^{-1} was covered using a sample-detector distance of 17.6 m for empty and loaded Psomes and 50% Dsomes at c_{BCP} = 0.2 mg/mL. Empty 100% Dsomes were measured for comparison. Quartz cuvettes with a pathlength of 2 cm have been used for measurements in D_2O, and with a pathlength of 1 cm for measurements in H_2O and H_2O:D_2O mixtures. The scattering intensities were recorded with a ^{3}He Reuter-Stokes multi-tube detector consisting of three panels with a total of 256 tubes with 256 pixels each. The pixel size is 4 mm along a tube and 8 mm due to the inner tube diameter. Received scattering curves were subtracted for solvent background and fitted using standard functions within SASview (https://www.sasview.org/). The investigated Psome samples were produced based on the procedures described in the literature.[5,6] 50% Dsomes were prepared by using a 1:1 mixture of conventional block copolymer and block copolymer with deuterated hydrophobic block for Psome formation. For 100% Dsomes solely the deuterated block-copolymer was used for particle formation. All loaded samples with cargo either of myoglobin (MYO), the enzyme hyaluronidase (HYAL), or gold nanoparticles (Au NPs) were post-loaded overnight at pH 6 directly before the measurements at ILL. Experiments were performed at pH 8 using 1 mM PBS buffer solutions. For experiments in D_2O, all used solvents have been replaced by their deuterated analogue, resulting in a D_2O solution containing Psomes or Dsomes, deuterated MYO with an estimated deuteration of 20%,[7] deuterated enzyme HYAL with an unknown fraction of deuteration, or Au NPs with deuterated hydration shell.

References

1 M. Kotlarchyk and S. H. Chen, *J. Chem. Phys.*, 1983, **79**, 2461–2469.
2 O. V. Tomchuk, L. A. Bulavin, V. L. Aksenov, V. M. Garamus, O. I. Ivankov, A. Y. Vul', A. T. Dideikin and M. V. Avdeev, *J. Appl. Crystallogr.*, 2014, **47**, 642–653.
3 P. Van Beurten and A. Vrij, *J. Chem. Phys.*, 1981, **74**, 2744–2748.
4 S. Moreno, S. Boye, A. Lederer, A. Falanga, S. Galdiero, S. Lecommandoux, B. Voit and D. Appelhans, *Biomacromolecules*, 2020, **21**, 5162–5172.
5 H. Gumz, S. Boye, B. Iyisan, V. Krönert, P. Formanek, B. Voit, A. Lederer and D. Appelhans, *Adv. Sci.*, 2019, **6**, 1801299.
6 E. Geervliet, S. Moreno, L. Baiamonte, R. Booijink, S. Boye, P. Wang, B. Voit, A. Lederer, D. Appelhans and R. Bansal, *J. Control. Release*, 2021, **332**, 594–607.
7 M. Palinske, U. L. Muza, S. Moreno, D. Appelhans, S. Boye, R. Schweins and A. Lederer, *Macromol. Chem. Phys.*, 2023, **244**, 2200300.